

# Neuronal activity and Wnt signaling act through Gsk3- $\beta$ to regulate axonal integrity in mature *Drosophila* olfactory sensory neurons

Albert Chiang<sup>1</sup>, Rashi Priya<sup>1</sup>, Mani Ramaswami<sup>2,3,4</sup>, K. VijayRaghavan<sup>1,\*</sup> and Veronica Rodrigues<sup>1,4,\*</sup>

The roles played by signaling pathways and neural activity during the development of circuits have been studied in several different contexts. However, the mechanisms involved in maintaining neuronal integrity once circuits are established are less well understood, despite their potential relevance to neurodegeneration. We demonstrate that maintenance of adult *Drosophila* olfactory sensory neurons requires cell-autonomous neuronal activity. When activity is silenced, development occurs normally, but neurons degenerate in adulthood. These detrimental effects can be compensated by downregulating Glycogen synthase kinase-3 $\beta$  (Gsk-3 $\beta$ ). Conversely, ectopic expression of activated Gsk-3 $\beta$  or downregulation of Wnt effectors also affect neuron stability, demonstrating a role for Wnt signaling in neuroprotection. This is supported by our observation that activated adult neurons are capable of increased Wingless release, and its targeted expression can protect neurons against degeneration. The role of Wnt signaling in this process is non-transcriptional, and may act on cellular mechanisms that regulate axonal or synaptic stability. Together, we provide evidence that Gsk-3 $\beta$  is a key sensor involved in neural circuit integrity, maintaining axon stability through neural activity and the Wnt pathway.

**KEY WORDS:** *Drosophila*, Olfactory system, Neuronal activity, Gsk-3 $\beta$  (Shaggy), Wingless

## INTRODUCTION

The steps in the development of a neuronal circuit require the specification of cellular components followed by morphogenesis into connectivity and function. There are several well-studied examples of the role of neuronal activity in embedding functional capabilities onto the final form of a circuit (Spitzer, 2006). The mature brain also continues to change through turnover and reorganization of neuronal branches and synapses. Here too, neuronal activity can effect changes in circuit properties and connectivity, forming the basis for learning and memory (Chklovskii et al., 2004). Signals other than neuronal activity are also able to alter mature neuronal circuits. For example, hormonal changes or stress can trigger major changes in brain regions, including the death of neurons (Truman and Riddiford, 2002) or growth of neuronal branches (Lamprecht and LeDoux, 2004). Thus, as in development, in the mature animal neurotrophic factors and activity are both involved in effecting changes in the brain. This plasticity of neural circuits in response to stimuli is balanced by homeostatic mechanisms that allow circuits to yield the same output in the face of random fluctuations in its activity or in environmental factors (Marder and Goaillard, 2006). The adult brain therefore is sculpted by a range of activity-dependent processes leading to synapse growth and elimination, although the underlying mechanisms remain poorly studied, particularly in vivo (Goda and Davis, 2003).

In this study, we ask whether the maintenance of neuron integrity is an active process and, if so, what are the cell-autonomous and non-autonomous mechanisms involved. In vertebrates, spontaneous activity functions to sculpt the final aspects of circuit synaptogenesis and maturation at the glomerular targets in the olfactory bulb (Yu et al., 2004). In addition, activity in sensory neurons is required for their maintenance, pointing to a relatively novel and unexplored activity-dependent neuronal phenomenon (Yu et al., 2004). We first established the *Drosophila* olfactory system as a preparation in which mechanisms underlying neuronal maintenance can be genetically analyzed in the context of its well-defined network. The olfactory system in *Drosophila* is perhaps one of the best-understood neural circuits in terms of its anatomy and function. There are ~1200 olfactory sensory neurons (OSNs) that project from the sense organs, which are located on the antennae and maxillary palps, to glomeruli within the antennal lobe (see Fig. 1A) (Laissue and Vosshall, 2008). Within each glomerulus, OSNs that express a specific odorant receptor (OR) gene synapse with excitatory and inhibitory local interneurons and projection interneurons that wire to the mushroom bodies and lateral protocerebrum. Such matching of OR expression in subsets of OSNs with defined second-order neurons to create a functional glomerular specificity has been observed in all insects and vertebrates examined (Komiya and Luo, 2006).

Here, we first confirm that, as in vertebrates (Yu et al., 2004), neural activity is necessary to maintain the integrity of adult *Drosophila* OSNs and then extend this knowledge by detailed characterization of temporal, cellular and molecular aspects of OSN maintenance. Cell-autonomous OSN phenotypes resulting from a lack of activity can be mimicked by inhibiting Wingless (Wg)/Wnt signaling and can be rescued by downregulating Gsk-3 $\beta$ , overexpressing Dishevelled (Dsh) or Wg, or by increasing the endogenous activity in OSNs. These and other observations indicate that neural activity and the Wg/Wnt signaling pathway collaborate to regulate Gsk-3 $\beta$  activity in the maintenance of OSN integrity. In

<sup>1</sup>National Centre for Biological Sciences, TIFR, GKVK Campus, Bangalore-65, India.

<sup>2</sup>Smurfit Institute of Genetics and TCIN, Lloyd Building, Trinity College Dublin, Dublin-2, Ireland. <sup>3</sup>Department of Molecular and Cellular Biology, University of Arizona, Tucson, AZ 85721, USA. <sup>4</sup>Department of Biological Sciences, Tata Institute of Fundamental Research, Homi Bhabha Road, Mumbai-5, India.

\*Authors for correspondence (e-mails: vijay@ncbs.res.in; veronica@ncbs.res.in)

mammals, the activation of Gsk-3 $\beta$  has been demonstrated to lead to Alzheimer's disease-related synaptic impairments (Liu et al., 2003; Zhu et al., 2007). We discuss the mechanisms and significance of this activity-dependent maintenance of the olfactory peripheral sensory map that acts through Gsk-3 $\beta$ .

## MATERIALS AND METHODS

### *Drosophila* strains

The OSN Gal4 lines *Or83b-Gal4*(11.17), *Or83b-Gal4* on III, *Or47b-Gal4*(15.7), *Or22a-Gal4*(14.21), *UAS-Or83b* and *Or83b*<sup>1</sup> and *Or83b*<sup>2</sup> null alleles (Benton et al., 2006; Larsson et al., 2004) were provided by Leslie Vosshall (Rockefeller University, New York, USA), *UAS-IMPTNT-V*, *UAS-TNT-G* by Sean Sweeney and Cahir O'Kane (University of York, UK and University of Cambridge, UK), *UAS-Kir2.1-EGFP* by Richard Baines (University of Manchester, UK), *UAS-2 $\times$ EGFP* by Haig Keshishian (Yale University, USA), *UAS-Wld<sup>8</sup>* by Marc Freeman (University of Massachusetts, USA), *UAS-dsh DN. $\Delta$ DIX* by Jeffrey Axelrod (Stanford University, USA) and *UAS-arrow  $\Delta$ C* from Jean-Paul Vincent [National Institute for Medical Research (MRC), UK]. *UAS-eag-DN*, *UAS-Sh-DN* is a double recombinant of previously described strains (Broughton et al., 2004; Mosca et al., 2005) from Subhabrata Sanyal. *UAS-p35*, *UAS-sgg DN. $\Delta$ 81T*, *UAS-sgg CA.S9A*, *UAS-Axn-GFP*, *UAS-shibire<sup>K44A</sup>*, *UAS-mCD8::GFP*, *UAS-pan.dTCFAN*, *UAS-arm.S10*, *FRT19A*, *FRT19A tub-Gal80* hsFlp, *UAS-dsh-myc*, *UAS-wg-HA*, *UAS-UBP2* and *tub-Gal80<sup>ts</sup>.tub-Gal80<sup>ts</sup>* recombinant stocks were obtained from the *Drosophila* Stock Center, Bloomington, IN, USA.

### Immunohistochemistry

Dissection and antibody staining of adult brain was carried out as described previously (Jhaveri et al., 2000). Primary antibodies used were 1:10 anti-Brp (DSHB), 1:50 mAb22C10 (DSHB), 1:10,000 rabbit anti-GFP (A6455, Molecular Probes), 1:1 anti-Wg (4D4, DSHB). Secondary antibodies used were Alexa 488 goat anti-rabbit, Alexa 568 goat anti-mouse and Alexa 647 goat anti-mouse (1:200, Molecular Probes). Labeled samples were mounted in 80% glycerol and imaged on an Olympus Fluoview FV1000 confocal microscope at 1  $\mu$ m intervals. Data were processed using ImageJ and pseudo-coloring and enhancements were implemented with Adobe Photoshop CS2. In all images, the right-hand antennal lobe is shown, with dorsal up and lateral to the left.

In order to test for Wg release, dissected brains were subjected to spaced 5 $\times$  K<sup>+</sup> depolarization (Ataman et al., 2008) by dissecting in normal HL3-saline (Stewart et al., 1994), then exposing to 90 mM KCl-HL3 solution for 5 minutes with gaps of 15 minutes in normal HL3-saline. Brains were fixed immediately after treatment and stained with anti-Wg antibody as described above. Pixel intensities were measured as described below and levels of immunoreactivity represented as a 'heat map'.

### Generation of MARCM clones

Late second instar larvae of a cross between *FRT19A*, *tub-Gal80*, *hsFlp*; *UAS-TNT-G/CyO* and *FRT19A*; *Or47b-Gal4*, *UAS-mCD8::GFP/CyO* (60–72 hours AEL) were heat shocked for 1 hour at 37°C to induce OSN clones that express mCD8::GFP and TNT-G and were compared with controls that expressed only mCD8::GFP.

### Quantitative confocal imaging

Samples were imaged at 1  $\mu$ m thickness at a frame size of 512 $\times$ 512 pixels under identical acquisition settings. Glomerular identification was aided by staining with anti-Brp and compared with glomerular maps (Couto et al., 2005; Laissue et al., 1999). To measure glomerular volume, contours of VA1v and VA6 were traced in individual sections (see Fig. S4H in the supplementary material), and volumes calculated by summation of individual areas in each section multiplied by the section thickness. GFP intensity was estimated in regions of interests (ROIs) (see green circles in Fig. S4F in the supplementary material) within the VA1v glomerulus. To quantify the pixel footprint of OSN terminals, a modification of a previously described method was used (Brown et al., 2006). ROIs in the GFP channel were traced to obtain the total number of pixels and the

intensity of each pixel. The background fluorescence intensity in the GFP channel was used to set the threshold to determine the total number of pixels showing GFP.

All measurements were manually traced with a virtual instrument written in LabVIEW 6.1 software (National Instruments). The values obtained were statistically analyzed, compared and plotted as histograms using the Origin 6.0 program (Microcal Software).

## RESULTS

### Development is normal, but maintenance of OSN terminals in the antennal glomeruli is affected, in *Or83b*-null mutants

The olfactory co-receptor *Or83b* is known to dimerize with canonical odorant receptors (ORs) to aid OR trafficking to the dendrites of OSNs (Larsson et al., 2004; Neuhaus et al., 2005). These heterodimers have recently been shown to form ligand-activated channels (Sato et al., 2008; Wicher et al., 2008). As expected, neurons lacking *Or83b* show no odor-evoked activity and a strongly diminished spontaneous activity (Larsson et al., 2004). These mutants therefore provide a system for investigating the role of neuronal activity during the development and maintenance of OSNs.

We examined the morphology of OSNs in mutants null for *Or83b* by driving green fluorescent protein (GFP) using *Or83b-Gal4* (*Or83b-Gal4*, *UAS-mCD8::GFP*; *Or83b*<sup>-/-</sup>). *Or83b-Gal4* drives GFP in ~80% of OSNs, allowing visualization of their sensory terminals in antennal glomeruli (Fig. 1B) and their axons in the outer nerve fiber layer (Fig. 1B'). In *Or83b* nulls, OSNs are indistinguishable from those of the wild type at emergence (data not shown), supporting previous conclusions that OSN targeting in *Drosophila* does not require neuronal activity (Dobritsa et al., 2003). This pattern remains unchanged up to 2 days post-eclosion (PE; Fig. 1C), but older mutant animals show defects in morphology of the OSNs, a phenotype clearly visible within 6 days PE (Fig. 1D). The sensory terminals (arrowheads in Fig. 1D) as well as axons (arrowheads in Fig. 1D') appear 'beaded', or 'blebbed', which are characteristics of axonal degeneration (Saxena and Caroni, 2007). We ruled out the possibility that the phenotypes are an artifact of a failure of GFP transport into the axons (Larsson et al., 2004) by staining brains for the neuron-specific microtubule-associated protein Futsch, which is recognized by the monoclonal antibody 22C10 (Fujita et al., 1982; Hummel et al., 2000). In these preparations, the axons in the outer nerve fiber layer were apparent as broad tracts running from the antennal nerve entry point to the antennal commissure in controls (see Fig. S1A in the supplementary material), and these were severely disrupted in experimental (*Or83b*-null) animals (see Fig. S1B in the supplementary material).

We focused on a subset of OSNs (~23–25) marked by *Or22a*>GFP that converge onto the DM2 glomerulus (Fig. 2A,A'). As with *Or83b*>GFP discussed above, these neurons were not detectably affected in 2-day-old mutants (Fig. 2B), with signs of degeneration becoming apparent by 4 days PE (arrow in Fig. 2C), and progressing further at 6 (Fig. 2D) and 8 (Fig. 2E) days PE, when the number of axons innervating the glomerulus was reduced compared with 2 days PE. This suggests that some axons are completely degenerated by 6 and 8 days PE, which was confirmed by measuring the pixel intensity in regions over the axon fascicles (see Fig. S2A–F and Table S6 in the supplementary material) ( $P < 0.005$ ). By 6 days PE, the cell bodies were still unaffected (see Fig. S2G–K in the supplementary material) ( $P > 0.05$ ), indicating that degeneration initiates at the terminals and progresses in a retrograde manner.

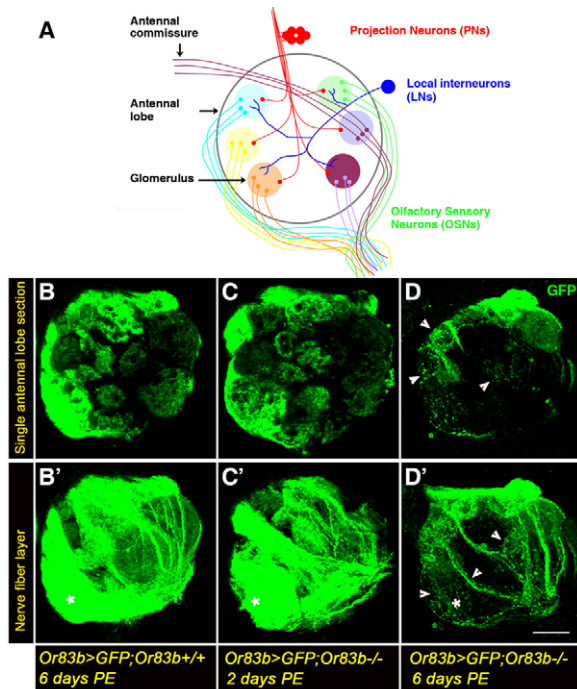


**Fig. 1. Development is normal, but maintenance of OSN terminals is affected, in *Or83b*-null mutants.** (A) Schematic of the olfactory system in adult *Drosophila*. The olfactory sensory neurons (OSNs) project to glomeruli within the antennal lobe, where they synapse with projection neurons (PNs) and local interneurons (LNs). Most OSNs send contralateral projections to the opposite antennal lobe, along the antennal commissure. (B-D') *Or83b*-Gal4-driven GFP expression labels the majority of the OSNs that innervate multiple glomeruli in the antennal lobe at 6 days (B,B'). In 2-day-old animals, the GFP pattern of *Or83b*-null animals (C,C') is comparable to that of wild type (B,B'), but degenerates in older animals (D,D'). B-D are single optical sections to show glomerular innervation by OSN axon terminals, and B'-D' are projections of five to ten of the anterior-most optical sections to highlight the OSN axons that make up the nerve fiber layer. Arrowheads in D,D' mark degenerating axons, which show characteristic blebbing and beading; the asterisk in B'-D' marks one of the broad nerve fiber tracts, which is severely disrupted in 6-day-old *Or83b*-null animals (D'). Genotypes: (B,B') *w*; *Or83b*-Gal4/*UAS-mCD8::GFP*; (C-D') *w*; *Or83b*-Gal4/*UAS-mCD8::GFP*; *Or83b*<sup>-/-</sup>. Scale bar: 25  $\mu$ m.

In order to test whether temporal expression of the *Or83b* protein could rescue these defects, we exploited the Gal80<sup>ts</sup> TARGET system (McGuire et al., 2003). Flies of genotype *Or22a*-Gal4, *UAS-mCD8::GFP/UAS-Or83b*; *tub*-Gal80<sup>ts</sup>, *Or83b*<sup>-/-</sup> were reared at 18°C (*Or83b*-OFF) and shifted to 29°C (*Or83b*-ON) at different times after eclosion. Phenotypes were examined at 8 days PE (Fig. 2F) and compared with age-matched mutants (Fig. 2E). Expression of the *Or83b* transgene beginning at eclosion (not shown) or 2 days PE resulted in a significant rescue of the defective phenotype when examined at 8 days (Fig. 2F, compare with 2E). The extent of rescue was quantified by estimating the pixel footprint of axonal terminals within the DM2 glomerulus (Brown et al., 2006). When targeted expression was initiated later (4 days PE), the rescue in glomerular arborization was also significant, although some blebbing in the axons still occurred (Fig. 2F',G; see Table S1 in the supplementary material) ( $P < 0.005$ ). *Or83b* expression beginning 6 days PE could not rescue the phenotype (Fig. 2F'',G; see Table S1 in the supplementary material) ( $P > 0.05$ ) because significant

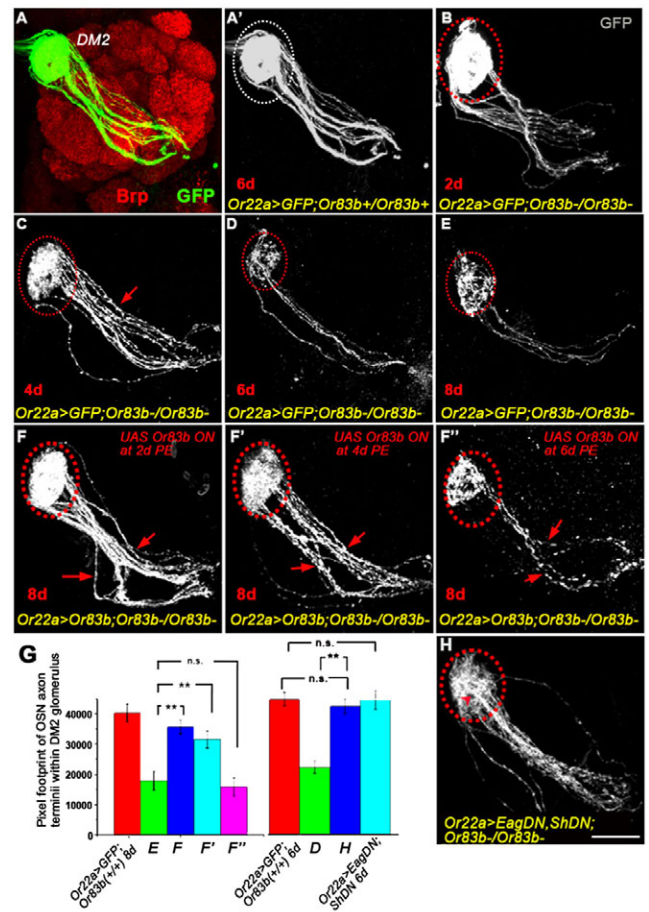


**Fig. 2. Maintenance of OSNs requires neuronal activity.**

(A) Antennal glomeruli stained with an antibody against Bruchpilot (Brp). (A') The *Or22a*-Gal4, *UAS-mCD8::GFP* line labels a set of ~23 OSNs that project to the DM2 glomerulus, shown here alone for clarity. (B-E) *Or83b*<sup>-/-</sup> flies with OSNs labeled by expression of GFP driven by *Or22a*-Gal4. These appear normal for the first 2 days PE (B), but show beading in the axons (arrow) by 4 days (C), which worsens to include the terminals (dotted lines) by 6 (D) and 8 (E) days PE. (F-F'') Conditional targeted expression of *Or83b* in *Or22a*-Gal4-expressing OSNs in *Or83b*<sup>-/-</sup> animals (*Or22a*-Gal4, *UAS-mCD8::GFP/UAS-Or83b*; *tub*-Gal80<sup>ts</sup>, *Or83b*<sup>-/-</sup>/*tub*-Gal80<sup>ts</sup>, *Or83b*<sup>-/-</sup>) for 2 (F), 4 (F'), or 6 (F'') days PE, and examined at 8 days PE in all cases. (G) Pixel intensities within the terminal arbors (demarcated by dotted lines) were estimated using LabVIEW 6.1 software and plotted as a bar chart (mean  $\pm$  s.e.m.,  $n=5$  in each case; for values, see Table S1 in the supplementary material). The letter below each bar indicates the figure in which the genotype being examined is shown. Data were subject to Student's unpaired *t*-test. \* $P < 0.05$ ; \*\* $P < 0.005$ ; n.s., not significant ( $P > 0.05$ ). (H) Induction of electrical activity within mutant *Or22a* OSNs by ectopic expression of *Eag*-DN and *Sh*-DN  $K^+$  channels. In G, the terminals (within dotted lines in H) were quantified (mean  $\pm$  s.e.m.) in 6-day-old animals; they show significant rescue (compared with D; see Table S2 in the supplementary material); \*\* $P < 0.005$ . Genotypes: (A,A') *Or22a*-Gal4, *UAS-mCD8::GFP*+/+; (B-E) *Or22a*-Gal4, *UAS-mCD8::GFP*+/+; *Or83b*<sup>-/-</sup>; (F-F'') *Or22a*-Gal4, *UAS-mCD8::GFP/UAS-Or83b*; *tub*-Gal80<sup>ts</sup>, *Or83b*<sup>-/-</sup>/*tub*-Gal80<sup>ts</sup>, *Or83b*<sup>-/-</sup>; (H) *Or22a*-Gal4, *UAS-mCD8::GFP/UAS-eag-DN*, *UAS-Sh-DN*; *Or83b*<sup>-/-</sup>. Scale bar: 20  $\mu$ m.

degeneration of neurons had already occurred. These results confirm a role for *Or83b* function in stabilizing adult neurons; replacement of the wild-type protein in mutants arrests further degeneration but cannot reverse effects that have already occurred. The current reagents

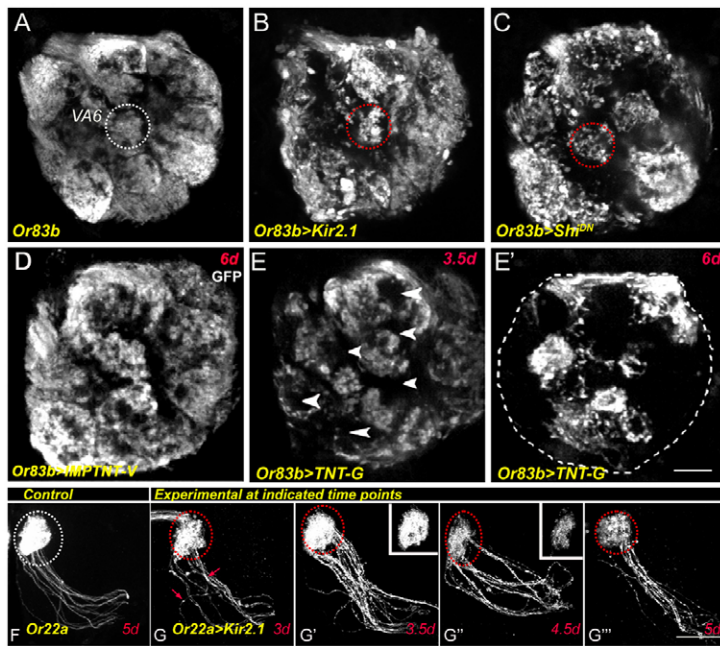


**Fig. 3. Effect of TNT-G, Kir<sub>2.1</sub> or Shi<sup>DN</sup> expression on the OSNs in the antennal lobe.** (A) Or83b OSNs in the normal *Drosophila* antennal lobe labeled with anti-GFP. The dotted line demarcates the VA6 glomerulus. (B,C) Conditional expression of Kir<sub>2.1</sub> (B) or Shi<sup>K44A</sup> (C) by Or83b-Gal4. (D-E') Or83b-Gal4-driven GFP used to visualize OSNs expressing either IMPTNT-V (D) or TNT-G (E, E'). Disruption of the presynaptic terminals is visible at 3.5 days PE (arrowheads in E), and becomes striking by 6 days PE (E'). (F-G''') Or22a OSNs terminating in DM2 visualized by anti-GFP (F). (G-G''') Kir<sub>2.1</sub> is expressed in adult Or22a OSNs. The neurodegeneration is progressive, starting at 3 days PE (G; arrows highlight beaded and fragmenting axons), and is extreme by 5 days PE (G'''). OSN terminals within the glomerulus are demarcated with dotted lines. Insets in G' and G''' show the terminals alone, for greater clarity. Genotypes: (A) *w; tub-Gal80<sup>TS</sup>, tub-Gal80<sup>TS</sup>/+; Or83b-Gal4, UAS-2×EGFP/+*; (B) *w; tub-Gal80<sup>TS</sup>, tub-Gal80<sup>TS</sup>/+; Or83b-Gal4, UAS-2×EGFP/UAS-Kir2.1*; (C) *w; tub-Gal80<sup>TS</sup>, tub-Gal80<sup>TS</sup>/+; Or83b-Gal4, UAS-2×EGFP/UAS-shi.K44A*; (D) *w; tub-Gal80<sup>TS</sup>, tub-Gal80<sup>TS</sup>/UAS-IMPTNT-V; Or83b-Gal4, UAS-2×EGFP/+*; (E, E') *w; tub-Gal80<sup>TS</sup>, tub-Gal80<sup>TS</sup>/UAS-TNT-G; Or83b-Gal4, UAS-2×EGFP/+*; (F) *Or22a-Gal4, UAS-mCD8::GFP/+; tub-Gal80<sup>TS</sup>, tub-Gal80<sup>TS</sup>/+*; (G-G''') *Or22a-Gal4, UAS-mCD8::GFP/+; tub-Gal80<sup>TS</sup>, tub-Gal80<sup>TS</sup>/UAS-Kir2.1*. Scale bars: 25 μm in A-E'; 20 μm in F-G''''.

do not allow us to delineate a critical period for Or83b requirement, if one exists; keeping Or83b on during development, but not after eclosion, prevented the degeneration normally observed at 6 days PE in mutants (see Fig. S3 and Table S7 in the supplementary material). However, these results are difficult to interpret given the presumed slow kinetics of the Gal4/Gal80<sup>TS</sup> system coupled with the undetermined stability of the Or83b protein.

Since Or83b is required for both odor-induced and spontaneous neural activity (Larsson et al., 2004), we examined whether the Or83b-null mutant phenotype could be rescued by induction of activity. Transgenic expression of dominant-negative (DN) *ether a go-go* (*eag*) or *Shaker* (*Sh*) K<sup>+</sup> channels have been shown to greatly enhance membrane excitability in neurons (Broughton et al., 2004; Mosca et al., 2005). We targeted expression of Eag-DN and Sh-DN channels into the Or22a-Gal4-expressing OSNs in Or83b-null mutant animals. Animals of the genotype *Or22a-Gal4, UAS-mCD8::GFP/UAS-eag-DN, UAS-Sh-DN; Or83b<sup>-/-</sup>*, were generated and the status of OSNs examined 6 days PE (Fig. 2H). A comparison of these neurons with those of mutants at the same age (Fig. 2D) showed a significant rescue of the defective phenotype, although some beading was still apparent in the axons; the extent of the terminal pixel footprint was comparable to that of normal animals (Fig. 2A', G; see Table S2 in the supplementary material) ( $P > 0.05$ ). We independently confirmed that ectopic expression of mutant K<sup>+</sup> channels did not result in altered terminal arborizations in wild-type neurons due to activity-dependent synaptic changes (Fig. 2G; see Table S2 in the supplementary material) ( $P > 0.05$ ).

These observations support the idea that neuronal activity, probably triggered by Or83b, is necessary for OSN survival in the adult. This suggests that blocking neuronal activity by other means might have effects similar to that seen in Or83b mutants.

### Neuronal activity and synaptic function are necessary for OSN stability in the adult olfactory system

The human inward rectifier K<sup>+</sup> channel (Kir<sub>2.1</sub>; KCNJ2 – HUGO) has been shown to hyperpolarize neuronal membranes, thereby inhibiting the generation of an action potential (Baines et al., 2001).

Flies carrying a UAS-Kir<sub>2.1</sub> transgene were crossed with Or83b-Gal4, UAS-2×EGFP, 2×*tub-Gal80<sup>TS</sup>* or Or22a-Gal4, UAS-mCD8::GFP, 2×*tub-Gal80<sup>TS</sup>*. Progeny were reared at 18°C until adulthood (Kir<sub>2.1</sub>-OFF). Newly eclosed flies were transferred to 29°C for 6 days (Kir<sub>2.1</sub>-ON), brains dissected and stained with antibodies to GFP and with the monoclonal antibody nc82, which recognizes the presynaptic protein Bruchpilot (Brp) (Wagh et al., 2006). OSNs 'silenced' by Kir<sub>2.1</sub> for 6 days PE showed a disruption of the glomerular pattern (Fig. 3B compared with 3A). We confirmed that the pattern was normal upon eclosion and until 3 days PE (data not shown). This phenotype could also be generated in a smaller subset of Or22a-Gal4-expressing neurons (Fig. 3G-G''' compared with 3F). The 'beaded' axon phenotype was apparent at 3 days PE (Fig. 3G) and became progressively more severe by 5 days PE (Fig. 3G''').

Silencing neurons by expression of Kir<sub>2.1</sub> inhibits the generation of action potentials, thus compromising both axonal conduction and synaptic release. We directly perturbed synaptic function by expression of a mutant Shikire protein (Shi<sup>K44A</sup>) that blocks synaptic vesicle recycling (Moline et al., 1999), or of the light chain of tetanus toxin (TeTxLC), which acts to enzymatically cleave neuronal synaptobrevin (n-Syb), thus abolishing evoked neurotransmitter release and causing a significant reduction in spontaneous release (Baines et al., 1999; Sweeney et al., 1995).

Adult-specific expression of either Shi<sup>K44A</sup> (Fig. 3C) or TeTxLC (TNT-G) (Fig. 3E, E') using the Or83b-Gal4 driver disrupted the integrity of OSNs, phenocopying the Or83b-null mutant defect. Degeneration was detected after 3.5 days PE (Fig. 3E) and became progressively more severe as the animal aged (Fig. 3E'). The cell bodies of the OSNs, however, were unaffected even after 6 days of treatment (see Fig. S2I-K in the supplementary material;  $P > 0.05$ ).

In these experiments, because we co-expressed GFP to monitor the status of the OSNs this lead to a possible concern that the phenotypes seen were artifacts of potentially reduced GFP levels when another transgene is introduced. The following observations argue against this possibility. First, there was no significant difference (see Fig. S4E and Table S8 in the supplementary material) ( $P > 0.05$ ) in the average fluorescence intensity of pixels highlighted

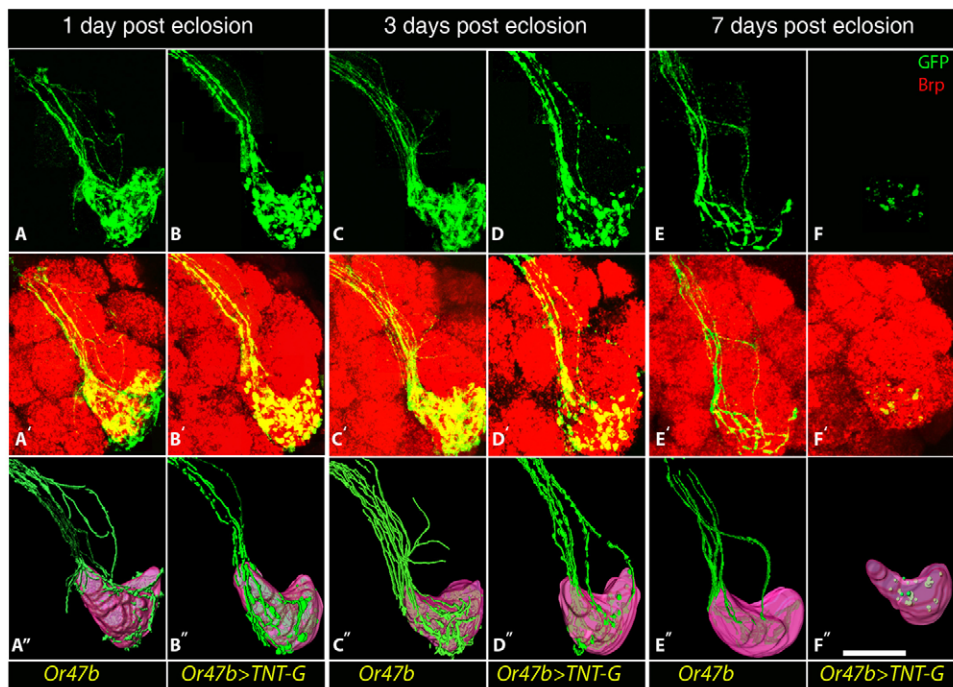


**Fig. 4. Maintenance of OSNs requires autonomous neuronal activity.**

(A-F'') *Or47b*-Gal4-driven GFP expression labels a subset of OSNs (~50) that innervate the VA1v glomerulus. Clones generated by MARCM label a subset of *Or47b*-Gal4-expressing OSNs. In B,D,F, clonal OSNs express TNT-G (and GFP, green in all panels), whereas the rest of the *OR47b* OSNs are unmarked and normal. Controls (A,C,E) and experimental (B,D,F) samples showing similar clone sizes were examined at 1 (A,B), 3 (C,D) and 7 (E,F) days PE. Samples were stained using anti-GFP (green; A-F) and anti-Brp (A'-F'). A''-F'' are three-dimensional reconstructed images of clonal cells (Amira 4.1 and 5.0). GFP-marked regions from consecutive confocal sections were selected and merged. Genotypes: (A,C,E) *FRT19A/FRT19A, tubGal80, hsFlp; Or47b-Gal4(15.7), UAS-mCD8::GFP/+*; (B,D,F) *FRT19A/FRT19A, tub-Gal80, hsFlp; Or47b-Gal4(15.7), UAS-mCD8::GFP/UAS-TNT-G*. Scale bar: 20  $\mu$ m.

by the GFP reporter in preparations in which a mutated and inactivated tetanus toxin (IMPTNT-V) was expressed (see Fig. S4A in the supplementary material) as compared with TNT-G (see Fig. S4C in the supplementary material). Second, the volume of VA1v, the target of *Or47b*-Gal4-expressing neurons, when expressed relative to that of the unaffected neighboring glomerulus VA6, was significantly reduced (see Fig. S4G and Table S8 in the supplementary material) ( $P < 0.005$ ) when TNT-G (see Fig. S4D in the supplementary material) but not IMPTNT-V (see Fig. S4B in the supplementary material) was expressed. Lastly, we confirmed that expression of TNT-G by *Or83b*-Gal4 disrupted the architecture of the nerve fiber layer by staining brains with mAb22C10 (see Fig. S1D compared with controls in S1C in the supplementary material).

These data further strengthen our conclusion that neuronal/synaptic activity is necessary for OSN axonal stability.

### Activity is autonomously required in OSNs for their maintenance and glial cells are able to respond to degenerating neurons

The requirement for normal synaptic release for maintenance of neurons raises the possibility that active neurons release neurotrophic factors required for survival. In such a scenario, we would expect these signals to be non-autonomous when the blocking of activity in a subset of neurons could be compensated by active neighbors. Above, we demonstrated that silencing OSNs that innervate a single glomerulus in an otherwise normal antennal lobe led to degeneration of these neurons (Fig. 3G-G''). Hence, non-autonomous cues, if any, cannot be transferred across glomeruli. We used the MARCM (Lee and Luo, 2001) technique to generate clones of silenced OSNs within a population of cells innervating a single glomerular target. Recombination induced by a heat shock-regulated Flip-recombinase (*hsFlp*) results in expression of TNT-G in a subset of neurons within the domain of expression of *Or47b*-Gal4 that targets the VA1v glomerulus. Control (*FRT19A/FRT19A, tub-Gal80, hsFlp; Or47b-Gal4, UAS-mCD8::GFP/+*) and experimental (*FRT19A/FRT19A tub-Gal80 hsFlp; Or47b-Gal4 UAS-mCD8::GFP/UAS-TNT-G*)

siblings with ~10-12 out of ~45 neurons 'silenced' are shown in Fig. 4. OSNs expressing TNT-G showed severe degeneration with age, and by 7 days PE only a few terminals were visible (Fig. 4B,D,F). We obtained a few clones in which an even smaller number of OSNs were silenced (see Fig. S5 in the supplementary material). In all these preparations, including clones in which only two cells were silenced (see Fig. S5C in the supplementary material), neurons degenerated despite the fact that the neighboring cells were normal. Together, these data strongly argue that OSNs have an autonomous requirement for activity to ensure their survival.

Caspase-dependent pathways of programmed cell death do not mediate the neurodegeneration we observe because co-expression of the pan-caspase inhibitor, baculovirus p35, did not alter the lesions induced by TNT-G or *Kir2.1* (see Fig. S6B,E compared with S6A,D in the supplementary material). The suggestion of a mechanism of axonal degeneration that is independent of cell death (Saxena and Caroni, 2007) is supported by the observation that axonal degeneration in *Or83b*-null animals in which activity was silenced did not involve the OSN soma, even 6 days PE (see Fig. S2G,H in the supplementary material) ( $P > 0.05$ ).

Studies by Freeman and colleagues (MacDonald et al., 2006) demonstrated that transection of the antennal nerve results in a process resembling the Wallerian degeneration elucidated in vertebrates. The *Wld<sup>S</sup>* transgene, which protects neurons against Wallerian degeneration, could not, however, rescue the phenotypes obtained upon TNT-G or *Kir2.1* expression (see Fig. S6C,F compared with S6A,D in the supplementary material). The degeneration does, however, require the proteasome degradative machinery because expression of the yeast ubiquitin-specific protease UBP2 (DiAntonio et al., 2001; Watts et al., 2003) protected *Or22a* neurons from degeneration in the *Or83b*-null background (see Fig. S6G-I and Table S4 in the supplementary material) ( $P < 0.005$ ).

Subsequent to degeneration, axon terminals were 'cleared' such that only GFP-marked remnants remained by 7 days PE (Fig. 4F). The levels of the glial phagocytic receptor Draper (MacDonald et al., 2006) were elevated in these regions (see Fig. S6N in the

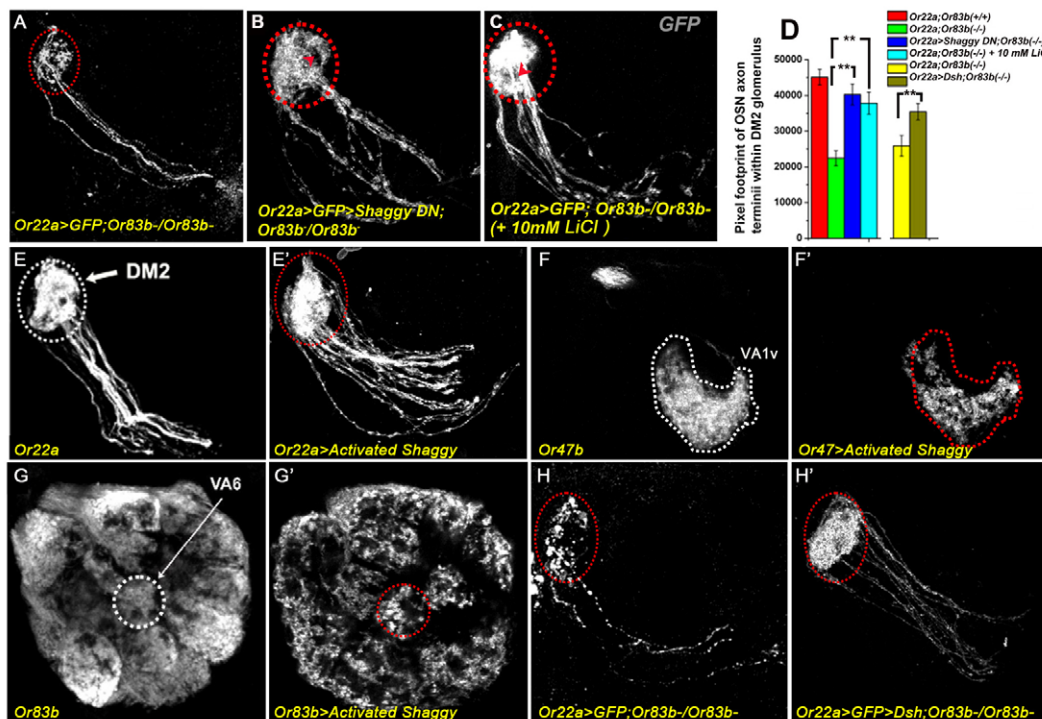


**Fig. 5. The state of Gsk-3 $\beta$  activation influences OSN stability.** (A) *Or22a*-Gal4, *UAS-mCD8::GFP*-marked OSNs in *Or83b*-null flies at 6 days PE. The control image shown in Fig. 2D is reproduced in A for ease of comparison. (B) Co-expression of a *sgg DN.A81T* transgene in mutant OSNs. (C) OSNs are rescued in mutants fed for 6 days with 10 mM LiCl. OSN terminals in a DM2 glomerulus (dotted lines; B,C) show reduced degeneration upon Gsk-3 $\beta$  inactivation as compared with age-matched controls (A). Arrowheads in B,C indicate gaps in the glomerular innervation of *Or22a*-Gal4 expressing OSNs at the DM2 glomerulus. (D) Pixel intensities in footprints (mean $\pm$ s.e.m.) of preparations shown in B and C ( $n=5$  each) are compared with A ( $n=5$ ) and with normal *Or22a*-Gal4, *UAS-mCD8::GFP* animals as shown in E ( $n=5$ ).  $**P<0.005$ . (E,E') *Or22a*-Gal4, *UAS-mCD8::GFP* (E) and with conditional expression of constitutively activated Gsk-3 $\beta$  (*UAS-sgg CA.S9A*) (E'). (F,F') *Or47b*-Gal4, *UAS-mCD8::GFP* (F) and with adult-specific expression of constitutively activated Gsk-3 $\beta$  (*UAS-sgg CA.S9A*) (F'). (G,G') *Or83b*-Gal4, *UAS-2 $\times$ EGFP* (G, the control image shown in Fig. 3A is reproduced in G for ease of comparison) and with constitutively activated Gsk-3 $\beta$  (*UAS-sgg CA.S9A*) (G'). Animals in E-G' are 6 days PE. (H,H') *Or22a*-Gal4, *UAS-mCD8::GFP*-marked OSNs in *Or83b*-null animals (H) and co-expressing *Dsh* (H'). The terminal arbors were assessed by measuring the pixels within the DM2 glomerulus (plotted in D,  $**P<0.005$ ). Samples in H were prepared in parallel (see Table S4 in the supplementary material). Genotypes: (A,C) *Or22a*-Gal4, *UAS-mCD8::GFP/+*; *Or83b<sup>-/-</sup>*; (B) *Or22a*-Gal4, *UAS-mCD8::GFP/UAS-sgg DN.A81T*; *Or83b<sup>-/-</sup>*; (E) *Or22a*-Gal4, *UAS-mCD8::GFP/+*; *tub-Gal80<sup>ts</sup>*, *tub-Gal80<sup>ts/+</sup>*; (E') *Or22a*-Gal4, *UAS-mCD8::GFP/+*; *tub-Gal80<sup>ts</sup>*, *tub-Gal80<sup>ts/UAS-sgg CA.S9A</sup>*; (F) *w*; *Or47b*-Gal4(15.7), *UAS-mCD8::GFP/+*; *tub-Gal80<sup>ts</sup>*, *tub-Gal80<sup>ts/+</sup>*; (F') *w*; *Or47b*-Gal4(15.7), *UAS-mCD8::GFP/+*; *tub-Gal80<sup>ts</sup>*, *tub-Gal80<sup>ts/UAS-sgg CA.S9A</sup>*; (G) *w*; *tub-Gal80<sup>ts</sup>*, *tub-Gal80<sup>ts/+</sup>*; *Or83b*-Gal4, *UAS-2 $\times$ EGFP/+*; (G') *w*; *tub-Gal80<sup>ts</sup>*, *tub-Gal80<sup>ts/+</sup>*; *Or83b*-Gal4, *UAS-2 $\times$ EGFP/UAS-sgg CA.S9A*; (H) *Or22a*-Gal4, *UAS-mCD8::GFP/+*; *Or83b<sup>-/-</sup>*; (H') *Or22a*-Gal4, *UAS-mCD8::GFP/+*; *UAS-dsh-myc*, *Or83b<sup>-/-</sup>Or83b<sup>-/-</sup>*.

supplementary material). Animals in which *Or47b* neurons were silenced (*Or47b*-Gal4, *UAS-mCD8::GFP/UAS-TNT-G*;  $2\times$ *tub-Gal80<sup>ts/+</sup>* shifted to 29°C) exhibited higher levels of Draper in the target glomerulus, VA1v, than controls (*Or47b*-Gal4, *UAS-mCD8::GFP/UAS-IMPNT-V*;  $2\times$ *tub-Gal80<sup>ts/+</sup>*) (see Fig. S6J-N and Table S8 in the supplementary material) ( $P<0.05$ ). Staining with the glial-specific marker Repo did not reveal an increase in cell number (data not shown). This means that extant glial cells upregulate Draper expression in response to degenerating OSNs.

### Downregulation of Glycogen synthase kinase-3 $\beta$ activity rescues degeneration in *Or83b* mutants

What are the mechanisms that are induced by activity in adult neurons? Studies of long-term potentiation (LTP) demonstrate that neuronal activity elevates the inhibitory phosphorylation of Gsk-3 $\beta$  [Shaggy (Sgg)] (Hooper et al., 2007). Further, altered Gsk-3 $\beta$  activity has been implicated in disease models of neural degeneration (Liu et al., 2003; Zhu et al., 2007). We reasoned that if neuronal activity impinged upon Gsk-3 $\beta$ , then inhibiting its activity could bypass the requirement for neuronal activity. A dominant-negative Gsk-3 $\beta$

construct (*UAS-sgg DN.A81T*) (Ataman et al., 2008; Bourouis, 2002) was targeted to the *Or22a* OSNs in *Or83b* homozygous null animals. When examined at 6 days PE, axons as well as presynaptic terminals showed significant rescue as compared with age-matched controls lacking the transgene (Fig. 5B compared with 5A,D; see Table S3 in the supplementary material) ( $P<0.005$ ). Hence, inhibition of Gsk-3 $\beta$  can compensate for neural activity and preserve neuronal integrity. Lithium chloride (LiCl) is a known pharmacological blocker of Gsk-3 $\beta$  activity (Kirshenboim et al., 2004). Feeding *Or83b*-null mutants with a 10 mM LiCl diet from immediately after eclosion resulted in a considerable rescue (Fig. 5C compared with 5A,D (see Table S3 in the supplementary material) ( $P<0.005$ ).

These observations indicate that neuronal activity mediates its effect by inhibiting the kinase activity of Gsk-3 $\beta$ . Consistent with such a model, constitutive activation of Gsk-3 $\beta$  resulted in phenotypes resembling that resulting from a lack of neuronal activity. Driving constitutively activated Gsk-3 $\beta$  (*UAS-sgg CA.S9A*) (Bourouis, 2002) for 6 days PE in *Or22a*, *Or47b* and *Or83b* adult OSNs using the inducible *Gal80<sup>ts</sup>* system (Fig. 5E-G) resulted in significant degeneration of presynaptic terminals (dotted lines in Fig. 5

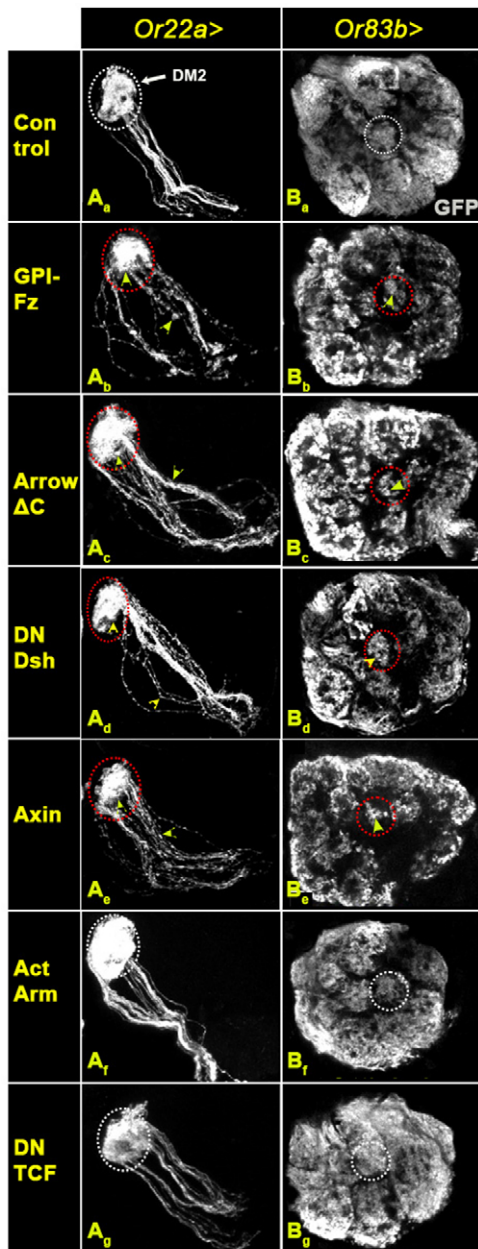


**Fig. 6. Perturbation of Wg/Wnt signaling leads to OSN degeneration.**

(Aa–Ag) *Or22a*-Gal4,UAS-*mCD8::GFP*-marked OSNs target to DM2. (Ba–Bg) *Or83b*-Gal4,UAS-2×*EGFP*-labeled OSNs (the control image shown in Fig. 3A is reproduced in Ba for ease of comparison). The *tub*-Gal80<sup>ts</sup> system was used to express GPI-fz (Ab,Bb), arrow  $\Delta$ C (Ac,Bc), *DN-dsh* (Ad,Bd), *Axin* (Ae, Be), activated *arm.S10* (Af,Bf) and *DN-dTCF* (Ag,Bg). All perturbations, except *Arm.S10* and *DN-dTCF*, show neurodegeneration. Genotypes: (Aa) *w*; *Or22a*-Gal4, UAS-*mCD8::GFP*+/+; *tub*-Gal80<sup>ts</sup>, *tub*-Gal80<sup>ts</sup>/+; (Ab) *w*; *Or22a*-Gal4, UAS-*mCD8::GFP*/UAS-*GPI-fz*+; *tub*-Gal80<sup>ts</sup>, *tub*-Gal80<sup>ts</sup>/+; (Ac) *w*; *Or22a*-Gal4, UAS-*mCD8::GFP*/UAS-*arrow*  $\Delta$ C; *tub*-Gal80<sup>ts</sup>, *tub*-Gal80<sup>ts</sup>/+; (Ad) *w*; *Or22a*-Gal4, UAS-*mCD8::GFP*/UAS-*dsh DN.ΔDIX*; *tub*-Gal80<sup>ts</sup>, *tub*-Gal80<sup>ts</sup>/+; (Ae) *w*; *Or22a*-Gal4, UAS-*mCD8::GFP*/UAS-*Axn-GFP*; *tub*-Gal80<sup>ts</sup>, *tub*-Gal80<sup>ts</sup>/+; (Af) *w*; UAS-*arm.S10*; *Or22a*-Gal4, UAS-*mCD8::GFP*+/+; *tub*-Gal80<sup>ts</sup>, *tub*-Gal80<sup>ts</sup>/+; (Ag) *w*; *Or22a*-Gal4, UAS-*mCD8::GFP*/UAS-*pan.dTCFΔN*; *tub*-Gal80<sup>ts</sup>, *tub*-Gal80<sup>ts</sup>/+; (Ba) *w*; *tub*-Gal80<sup>ts</sup>, *tub*-Gal80<sup>ts</sup>/+; *Or83b*-Gal4, UAS-2×*EGFP*+/+; (Bb) *w*; *tub*-Gal80<sup>ts</sup>, *tub*-Gal80<sup>ts</sup>/UAS-*GPI-fz*+; *Or83b*-Gal4, UAS-2×*EGFP*+/+; (Bc) *w*; *tub*-Gal80<sup>ts</sup>, *tub*-Gal80<sup>ts</sup>/UAS-*arrow*  $\Delta$ C; *Or83b*-Gal4, UAS-2×*EGFP*+/+; (Bd) *w*; *tub*-Gal80<sup>ts</sup>, *tub*-Gal80<sup>ts</sup>/UAS-*dsh DN.ΔDIX*; *Or83b*-Gal4, UAS-2×*EGFP*+/+; (Be) *w*; *tub*-Gal80<sup>ts</sup>, *tub*-Gal80<sup>ts</sup>/UAS-*Axn-GFP*; *Or83b*-Gal4, UAS-2×*EGFP*+/+; (Bf) *w*; UAS-*arm.S10*; *tub*-Gal80<sup>ts</sup>, *tub*-Gal80<sup>ts</sup>/+; *Or83b*-Gal4, UAS-2×*EGFP*+/+; (Bg) *w*; *tub*-Gal80<sup>ts</sup>, *tub*-Gal80<sup>ts</sup>/UAS-*pan.dTCFΔN*; *Or83b*-Gal4, UAS-2×*EGFP*+/+.

expressed in the *Or22a* OSNs (*w*; *Or22a*-Gal4, UAS-*mCD8::GFP*/UAS-*GPI-fz*+; *tub*-Gal80<sup>ts</sup>, *tub*-Gal80<sup>ts</sup>/+), or in *Or83b* OSNs during adulthood, axons and their terminals showed characteristic signs of degeneration (Fig. 6Ab,Bb compared with 6Aa,Ba). Further, perturbation of Arrow co-receptor function by expression of a truncated protein (Arrow  $\Delta$ C) (Fig. 6Ac,Bc) (Piddini et al., 2005), or a dominant-negative (DN) form of *dsh* (*dsh DN.ΔDIX*) (Fig. 6Ad,Bd) (Axelrod et al., 1998), or by overexpression of Axin (Cliffe et al., 2003) (Fig. 6Ae,Be) also caused neurodegeneration.

In the canonical Wg/Wnt pathway, the Axin-Apc-Gsk-3 $\beta$  complex acts to stabilize  $\beta$ -catenin, leading to transcriptional effects (Logan and Nusse, 2004). In our studies, expression of an activated form of  $\beta$ -catenin [activated Armadillo (Arm)] (Pai et al., 1997) (Fig. 6Af,Bf) or of a dominant-negative form of *Drosophila* TCF (dTCF; Pangolin) (DN-dTCF) (Fig. 6Ag,Bg) (van de Wetering et al., 1997) for 6 days did not compromise neuronal stability. These experiments together indicate that signaling downstream of Gsk-3 $\beta$ /Axin does not occur through transcriptional events mediated by dTCF. The end-point of Wg/Wnt signaling is therefore likely to be non-transcriptional and to involve a cytoplasmic role of Gsk-3 $\beta$  in regulating axon stability. This mechanism requires detailed investigation.

These results together lead to the hypothesis that Wnt signaling through Gsk-3 $\beta$  confers neuronal stability, which could have effects at synapses through the divergent canonical pathway (Ataman et al., 2008; Miech et al., 2008; Salinas, 2007; Speese and Budnik, 2007). Is there a link between neuronal activity and Wg signaling? Immunostaining of adult antennal lobes showed low Wg levels in glomeruli (Fig. 7A; see Fig. S7 in the supplementary material). Global activation of neurons by KCl-induced spaced depolarization (Ataman et al., 2008) led to a significant increase in Wg levels within the antennal glomeruli (Fig. 7B compared with 7A; see Table S5 in the supplementary material) ( $P < 0.005$ ). These data do not provide sufficient

E',F',G' compared with 5E,F,G) and axons. Gsk-3 $\beta$  is a known sensor for several different signaling pathways; regulation via the Wnt pathway is mediated by the cytoplasmic phosphoprotein Dsh, which signals to the Axin-Apc-Gsk-3 $\beta$  complex (Logan and Nusse, 2004). Ectopic expression of Dsh (Penton et al., 2002) protected the *Or22a* OSNs of *Or83b*-null animals from degeneration, even in 6-day-old animals (Fig. 5H,H'; see Table S4 in the supplementary material) ( $P < 0.005$ ). It is known that increased levels of Dsh can trigger Wnt signaling and lead to an inhibition of Gsk-3 $\beta$  activity (Ciani et al., 2004). This provides further evidence for the role of Wnt signaling in conferring neuronal stability.

### Wg/Wnt signaling regulates neuronal stability in the adult olfactory system

Ectopic expression of a membrane-tethered form of the Wg/Wnt receptor Frizzled (GPI-Fz) binds ligands in the vicinity of the cell and interferes with normal signaling (Rulifson et al., 2000). When

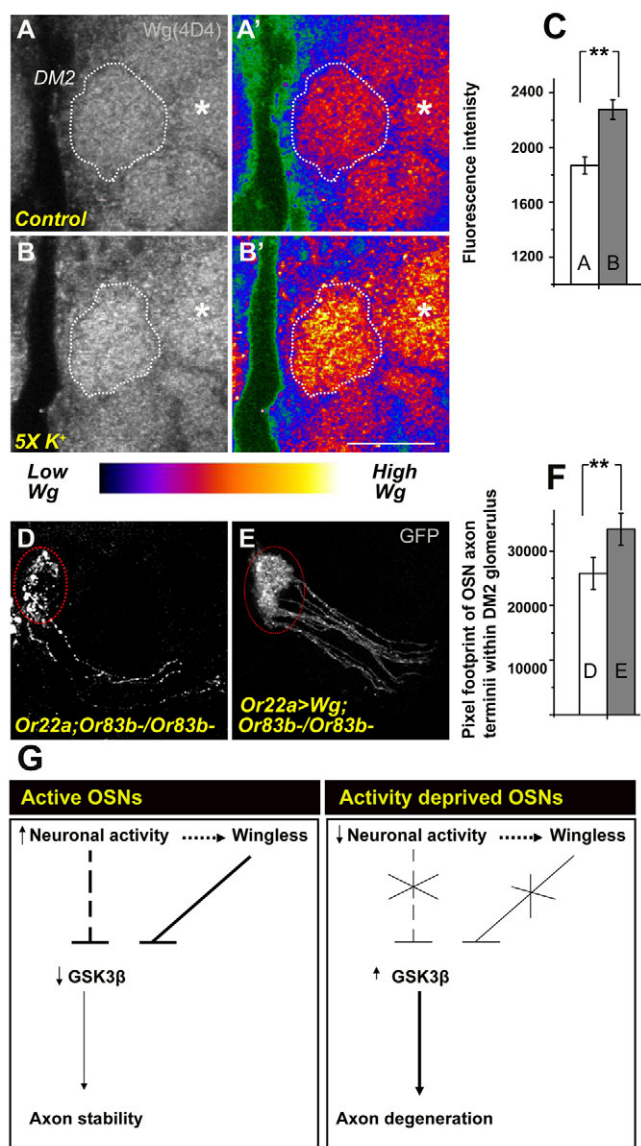


**Fig. 7. Intersection of neuronal activity, Gsk-3 $\beta$  and Wg signaling in conferring stability on adult OSNs.** (A-B') Adult *Drosophila* antennal lobes stained with anti-Wg antibody; the DM2 glomerulus is circled with a dotted line. Control brains (A) and brains depolarized by spaced  $5\times K^+$  exposure (B). Levels of immunoreactivity are represented by the colors of the heat map (A',B'). Asterisks highlight the glomerulus neighboring DM2, which also shows a significant increase in Wg levels compared with the control. (C) Mean pixel intensity  $\pm$ s.e.m. in control (A) and stimulated (B) DM2 glomeruli (identified by Or22a>GFP expression) was estimated and plotted (\*\* $P<0.005$ ). (D) Or22a OSNs labeled in the *Or83b*<sup>-/-</sup> mutants. The image shown in Fig. 5H is shown here again for ease of comparison. (E) Conditional targeted expression of Wg in the Or22a neurons results in rescue from degeneration. (F) Pixel intensities of the terminal arbors of controls (D) and experimental samples (E) show a significant difference (mean $\pm$ s.e.m.; \*\* $P<0.005$ ) (see Table S4 in the supplementary material). (G) In normal adult OSNs, Or83b-dependent neuronal activity leads to a release of Wg, which activates signaling leading to inhibition of Gsk-3 $\beta$ . Gsk-3 $\beta$  acts through a non-transcriptional pathway to stabilize axons/synapses. Neuronal activity could also impinge on Gsk-3 $\beta$  through Wg-independent pathways (represented by dotted lines). Genotypes: (A-B') *w*; Or22a-Gal4, UAS-*mCD8::GFP*+/+; (D) Or22a-Gal4, UAS-*mCD8::GFP*+/+; Or83b<sup>-/-</sup>; (E) Or22a-Gal4, UAS-*mCD8::GFP/UAS-wg*; Or83b<sup>-/-</sup>. Scale bar: 15  $\mu$ m in A-B'.

resolution to decipher whether Wg is released from the OSNs themselves or non-autonomously from the antennal lobe interneurons as a consequence of their activation.

We ectopically expressed Wg (Hays et al., 1997) in the Or22a OSNs in *Or83b*-null animals during adulthood and examined animals 6 days PE (Fig. 7E). Careful examination of the footprint of the Or22a terminals in the DM2 glomerulus indicated significant rescue of the degeneration as compared with control animals (Fig. 7D; see Table S4 in the supplementary material, plotted in Fig. 7F) ( $P<0.005$ ). This suggests that autocrine signaling by Wg does, at least in part, confer neuroprotection to the OSNs.

## DISCUSSION

During development, electrical activity and cell signaling pathways have been shown to collaborate to eliminate neurons or synaptic connections (Cohen-Cory, 2002; Spitzer, 2006). In the mature vertebrate nervous system, many neurons are eliminated, although the majority survive through the life of the animal. Little is known about the mechanisms underlying the maintenance of mature neurons in a circuit, or, indeed, whether there is any active requirement at all for maintenance. Given the fundamental role of electrical activity in neuronal function, we asked whether it is the sensor for the integrity of the nerve cell. In order to test this rigorously, we needed to have a preparation from which both spontaneous and evoked activity could be removed and the consequences on neuronal maintenance assessed. The OSNs are unique in that they allow the manipulation of spontaneous and odor-induced activity in the mature animal. Our experiments in this system implicate a role for activity in neuronal maintenance. Further, we show that Gsk-3 $\beta$ , a molecule that is a sensor for nutrients and Wnt signals (Grimes and Jope, 2001), acts 'downstream' of neuronal activity in this process. Our results thus integrate a key property of neurons, electrical activity, with Gsk-3 $\beta$  signaling (summarized in Fig. 7G). Although Gsk-3 $\beta$  can receive inputs from a variety of pathways, the expression of Wg in the adult antennal lobe and the observation that degeneration could be rescued by expression of Dsh and Wg, suggested that this is a major signaling pathway acting on neuronal survival in the mature animal. We also established that Wnt signaling acts through a non-transcriptional pathway involving Gsk-3 $\beta$ . The action of Wnt signaling during the formation and plasticity of neuronal circuits is mediated through the 'divergent canonical pathway', as demonstrated by several studies in both vertebrates and *Drosophila* (Ataman et al., 2008; Hall et al., 2000; Miech et al., 2008; Packard et al., 2002).

### Neuronal activity in the maintenance of integrity: autonomy at the sub-glomerular level

Gogos and colleagues have demonstrated that spontaneous activity is essential for both the development and maintenance of OSN projections in the mouse olfactory bulb (Cao et al., 2007; Yu et al., 2004). In *Drosophila*, the formation of the peripheral olfactory map is independent of ORs or activity, and is possibly hardwired (Dobritsa et al., 2003). However, as in mammals, OSN maintenance requires neural activity. We have exploited the availability of *Or83b*-null mutants and the conditional TARGET system (McGuire et al., 2003) to demonstrate that OSN terminals within the antennal lobe glomeruli develop normally in the absence of activity, but show local degeneration in older animals in which the most distal ends exhibit signs of beading, blebbing and, eventually, fragmentation, which are hallmarks of axon degeneration (Saxena and Caroni, 2007).

In vertebrates, electrically silent visual system neurons (Hua et al., 2005) and OSNs (Zhao and Reed, 2001) retract when placed in an environment of active neurons because of synaptic competition for target sites. When all neurons in a given field are silenced to the same extent, elimination does not occur, suggesting that differences in activity, rather than the absolute activity state, determine the stability of connections. Contrary to expectation from these findings, neurons innervating a single glomerulus retracted their contacts and showed degeneration when silenced. Further, clones that drive TNT-G in small subsets of OSNs also degenerate, indicating that activity influences neuron survival by exerting autonomous effects at the level of individual cells.

### Gsk-3 $\beta$ as a key sensor of inputs for neural activity and Wnt signaling in maintaining circuit stability

Enhanced neuronal activity has been shown to trigger the activation of a wide range of genes including transcription factors, cell adhesion molecules, membrane excitability proteins (Guan et al., 2005), translational regulators such as dFmr (Fmr1) (Tessier and Broadie, 2008) and signaling molecules such as Wnt (Ataman et al., 2008). Our observation that Wg is expressed in the adult brain led us to test the role of Wg/Wnt signaling in stability. We found that downregulation of Wg pathway members compromises OSN stability, resulting in phenotypes similar that resulting from a lack of neuronal activity. Several studies argue for a link between neuronal activity and Wnt/Wg signaling during formation of LTP (Ahmad-Annur et al., 2006; Chen et al., 2006) and in activity-dependent dendritic morphogenesis (Wayman et al., 2006; Yu and Malenka, 2003). At the *Drosophila* neuromuscular junction, activity-dependent Wg secretion results in structural outgrowth mediated by Gsk-3 $\beta$  in the motoneurons and nuclear localization of the cleaved C terminus of DFz2 in the postsynaptic muscle cells (Ataman et al., 2008).

We have provided evidence for a requirement of Wg/Wnt signaling for stabilization of adult OSNs, although a transcriptional output of the pathway is not required. Non-transcriptional roles for Wnt signaling have been demonstrated previously, well-studied examples being in Wnt7a-induced growth cone and axon remodeling of the mossy fibers (Hall et al., 2000) and in *Drosophila* neuromuscular junction synaptogenesis and plasticity (Ataman et al., 2008; Packard et al., 2002). The output of signaling in these systems is mediated by Gsk-3 $\beta$ , which regulates microtubule cytoskeletons. Gsk-3 $\beta$  phosphorylates the Microtubule-associated protein 1B (mammalian homolog of Futsch) and Tau, thereby influencing microtubule stability (Goold and Gordon-Weeks, 2004). Neuronal activity regulates Gsk-3 $\beta$  enzymatic activity through a series of phosphorylation and dephosphorylation events (Hooper et al., 2007; Peineau et al., 2007), whereby activity-regulated PP1 phosphatase and PI3K-Akt kinase regulate phosphorylation of Gsk-3 $\beta$  serine 9.

Activation of Gsk-3 $\beta$  in rat hippocampus inhibits LTP with associated synaptic impairments reminiscent of Alzheimer's disease (Liu et al., 2003; Zhu et al., 2007). A genetic link between late-onset Alzheimer's disease and the Wnt pathway co-receptor LRP6 has been demonstrated in human subjects (De Ferrari et al., 2007) and there is a possibility that Alzheimer's disease-associated synaptic impairments are due to aberrant GSK-3 $\beta$  kinase activity (Liu et al., 2003; Zhu et al., 2007). The phenotypes we observed in OSNs with activated Gsk-3 $\beta$  or a chronic blockage of activity are tantalizingly similar to those described during neurodegeneration in Alzheimer's disease models (Inestrosa and Toledo, 2008; Toledo et al., 2008).

We propose a model whereby neuronal activity acts together with Gsk-3 $\beta$  to maintain circuit stability in the adult olfactory system (Fig. 7G). Activity appears to lead to Wg release, which acts in an autocrine

manner to impinge upon Gsk-3 $\beta$  activity. It is also possible that autonomous activity could signal to Gsk-3 $\beta$  through other pathways, one of them being the energy status of the neuron (Grimes and Jope, 2001). In adult OSNs, Wnt signaling appears to be non-transcriptional and Gsk-3 $\beta$  possibly acts cell-autonomously to regulate the dynamics of the microtubule cytoskeleton (Salinas, 2007). Our results support the emerging view of a role for the Wnt pathway in neuroprotection, and our approach provides a system in which to examine the structural and molecular mechanisms that operate during altered physiological states in a genetically tractable organism.

We thank Leslie Vosshall, Sean Sweeney, Richard Baines, Francois Rouyer, Cahir O'Kane, Marc Freeman, Subhabrata Sanyal, Jeff Axelrod, Jean-Paul Vincent, Roel Nusse, Haig Keshishian, the *Drosophila* Stock Center (Indiana University) and DSHB (University of Iowa) for fly strains and antibodies. We acknowledge Aprotim Mazumder for inputs on the LabVIEW software, and Upinder Bhalla for comments on the manuscript. This work was supported by core funding from NCBS, TIFR; the Department of Biotechnology (K.V.R.); Science Foundation of Ireland (M.R.); and NIDA grant DA15495 associated Supplement for International Collaboration (V.R. and M.R.). We also acknowledge the Centre for Nanotechnology (Department of Science and Technology grant SR/S5/NM-36/2005) for use of the Olympus FV1000 microscopes in the CIFF and NOMIC imaging facility (NCBS). The authors have declared no competing interests. Deposited in PMC for release after 12 months.

#### Supplementary material

Supplementary material for this article is available at <http://dev.biologists.org/cgi/content/full/136/8/1273/DC1>

#### References

- Ahmad-Annur, A., Ciani, L., Simeonidis, I., Herreros, J., Fredj, N. B., Rosso, S. B., Hall, A., Brickley, S. and Salinas, P. C. (2006). Signaling across the synapse: a role for Wnt and Dishevelled in presynaptic assembly and neurotransmitter release. *J. Cell Biol.* **174**, 127-139.
- Ataman, B., Ashley, J., Gorczyca, M., Ramachandran, P., Fouquet, W., Sigrist, S. J. and Budnik, V. (2008). Rapid activity-dependent modifications in synaptic structure and function require bidirectional Wnt signaling. *Neuron* **57**, 705-718.
- Axelrod, J. D., Miller, J. R., Shulman, J. M., Moon, R. T. and Perrimon, N. (1998). Differential recruitment of Dishevelled provides signaling specificity in the planar cell polarity and Wingless signaling pathways. *Genes Dev.* **12**, 2610-2622.
- Baines, R. A., Robinson, S. G., Fujioka, M., Jaynes, J. B. and Bate, M. (1999). Postsynaptic expression of tetanus toxin light chain blocks synaptogenesis in *Drosophila*. *Curr. Biol.* **9**, 1267-1270.
- Baines, R. A., Uhler, J. P., Thompson, A., Sweeney, S. T. and Bate, M. (2001). Altered electrical properties in *Drosophila* neurons developing without synaptic transmission. *J. Neurosci.* **21**, 1523-1531.
- Benton, R., Sachse, S., Michnick, S. W. and Vosshall, L. B. (2006). Atypical membrane topology and heteromeric function of *Drosophila* odorant receptors in vivo. *PLoS Biol.* **4**, e20.
- Bourouis, M. (2002). Targeted increase in shaggy activity levels blocks wingless signaling. *Genesis* **34**, 99-102.
- Broughton, S. J., Kitamoto, T. and Greenspan, R. J. (2004). Excitatory and inhibitory switches for courtship in the brain of *Drosophila melanogaster*. *Curr. Biol.* **14**, 538-547.
- Brown, H. L. D., Cherbas, L., Cherbas, P. and Truman, J. W. (2006). Use of time-lapse imaging and dominant negative receptors to dissect the steroid receptor control of neuronal remodeling in *Drosophila*. *Development* **133**, 275-285.
- Cao, L., Dhillia, A., Mukai, J., Blazeski, R., Lodovichi, C., Mason, C. A. and Gogos, J. A. (2007). Genetic modulation of BDNF signaling affects the outcome of axonal competition in vivo. *Curr. Biol.* **17**, 911-921.
- Chen, J., Park, C. S. and Tang, S. J. (2006). Activity-dependent synaptic Wnt release regulates hippocampal long term potentiation. *J. Biol. Chem.* **281**, 11910-11916.
- Chklovskii, D. B., Mel, B. W. and Svoboda, K. (2004). Cortical rewiring and information storage. *Nature* **431**, 782-788.
- Ciani, L., Krylova, O., Smalley, M. J., Dale, T. C. and Salinas, P. C. (2004). A divergent canonical WNT-signaling pathway regulates microtubule dynamics: dishevelled signals locally to stabilize microtubules. *J. Cell Biol.* **164**, 243-253.
- Cliffe, A., Hamada, F. and Bienz, M. (2003). A Role of dishevelled in relocating axin to the plasma membrane during wingless signaling. *Curr. Biol.* **13**, 960-966.
- Cohen-Cory, S. (2002). The developing synapse: construction and modulation of synaptic structures and circuits. *Science* **298**, 770-776.
- Couto, A., Alenius, M. and Dickson, B. J. (2005). Molecular, anatomical, and functional organization of the *Drosophila* olfactory system. *Curr. Biol.* **15**, 1535-1547.

- De Ferrari, G. V., Papassotiropoulos, A., Biechele, T., Wavrant De-Vrieze, F., Avila, M. E., Major, M. B., Myers, A., Saez, K., Henriquez, J. P., Zhao, A. et al. (2007). Common genetic variation within the low-density lipoprotein receptor-related protein 6 and late-onset Alzheimer's disease. *Proc. Natl. Acad. Sci. USA* **104**, 9434-9439.
- DiAntonio, A., Haghighi, A. P., Portman, S. L., Lee, J. D., Amaranto, A. M. and Goodman, C. S. (2001). Ubiquitination-dependent mechanisms regulate synaptic growth and function. *Nature* **412**, 449-452.
- Dobritsa, A. A., van der Goes van Naters, W., Warr, C. G., Steinbrecht, R. A. and Carlson, J. R. (2003). Integrating the molecular and cellular basis of odor coding in the Drosophila antenna. *Neuron* **37**, 827-841.
- Fujita, S. C., Zipursky, S. L., Benzer, S., Ferrus, A. and Shotwell, S. L. (1982). Monoclonal antibodies against the Drosophila nervous system. *Proc. Natl. Acad. Sci. USA* **79**, 7929-7933.
- Goda, Y. and Davis, G. W. (2003). Mechanisms of synapse assembly and disassembly. *Neuron* **40**, 243-264.
- Goold, R. G. and Gordon-Weeks, P. R. (2004). Glycogen synthase kinase 3beta and the regulation of axon growth. *Biochem. Soc. Trans.* **32**, 809-811.
- Grimes, C. A. and Jope, R. S. (2001). The multifaceted roles of glycogen synthase kinase 3beta in cellular signaling. *Prog. Neurobiol.* **65**, 391-426.
- Guan, Z., Saraswati, S., Adolfsen, B. and Littleton, J. T. (2005). Genome-wide transcriptional changes associated with enhanced activity in the Drosophila nervous system. *Neuron* **48**, 91-107.
- Hall, A. C., Lucas, F. R. and Salinas, P. C. (2000). Axonal remodeling and synaptic differentiation in the cerebellum is regulated by WNT-7a signaling. *Cell* **100**, 525-535.
- Hays, R., Gabori, G. B. and Bejsovec, A. (1997). Wingless signaling generates pattern through two distinct mechanisms. *Development* **124**, 3727-3736.
- Hooper, C., Markevich, V., Plattner, F., Killick, R., Schofield, E., Engel, T., Hernandez, F., Anderson, B., Rosenblum, K., Bliss, T. et al. (2007). Glycogen synthase kinase-3 inhibition is integral to long-term potentiation. *Eur. J. Neurosci.* **25**, 81-86.
- Hua, J. Y., Smear, M. C., Baier, H. and Smith, S. J. (2005). Regulation of axon growth in vivo by activity-based competition. *Nature* **434**, 1022-1026.
- Hummel, T., Krukkert, K., Roos, J., Davis, G. and Klambt, C. (2000). Drosophila Futsch/22C10 is a MAP1B-like protein required for dendritic and axonal development. *Neuron* **26**, 357-370.
- Inestrosa, N. C. and Toledo, E. M. (2008). The role of Wnt signaling in neuronal dysfunction in Alzheimer's disease. *Mol. Neurodegener.* **3**, 9.
- Jhaveri, D., Sen, A. and Rodrigues, V. (2000). Mechanisms underlying olfactory neuronal connectivity in Drosophila: the atonal lineage organizes the periphery while sensory neurons and glia pattern the olfactory lobe. *Dev. Biol.* **226**, 73-87.
- Kirshenboim, N., Plotkin, B., Shlomo, S. B., Kaidanovich-Beilin, O. and Eldar-Finkelman, H. (2004). Lithium-mediated phosphorylation of glycogen synthase kinase-3beta involves PI3 kinase-dependent activation of protein kinase C-alpha. *J. Mol. Neurosci.* **24**, 237-245.
- Komiyama, T. and Luo, L. (2006). Development of wiring specificity in the olfactory system. *Curr. Opin. Neurobiol.* **16**, 67-73.
- Laissue, P. P. and Vosshall, L. B. (2008). The olfactory sensory map in Drosophila. *Adv. Exp. Med. Biol.* **628**, 102-114.
- Laissue, P. P., Reiter, C., Hiesinger, P. R., Halter, S., Fischbach, K. F. and Stocker, R. F. (1999). Three-dimensional reconstruction of the antennal lobe in Drosophila melanogaster. *J. Comp. Neurol.* **405**, 543-552.
- Lamprecht, R. and LeDoux, J. (2004). Structural plasticity and memory. *Nat. Rev. Neurosci.* **5**, 45-54.
- Larsson, M. C., Domingos, A. I., Jones, W. D., Chiappe, M. E., Amrein, H. and Vosshall, L. B. (2004). Or83b encodes a broadly expressed odorant receptor essential for Drosophila olfaction. *Neuron* **43**, 703-714.
- Lee, T. and Luo, L. (2001). Mosaic analysis with a repressible cell marker (MARCM) for Drosophila neural development. *Trends Neurosci.* **24**, 251-254.
- Liu, S. J., Zhang, A. H., Li, H. L., Wang, Q., Deng, H. M., Netzer, W. J., Xu, H. and Wang, J. Z. (2003). Overactivation of glycogen synthase kinase-3 by inhibition of phosphoinositol-3 kinase and protein kinase C leads to hyperphosphorylation of tau and impairment of spatial memory. *J. Neurochem.* **87**, 1333-1344.
- Logan, C. Y. and Nusse, R. (2004). The Wnt signaling pathway in development and disease. *Annu. Rev. Cell Dev. Biol.* **20**, 781-810.
- MacDonald, J. M., Beach, M. G., Porpiglia, E., Sheehan, A. E., Watts, R. J. and Freeman, M. R. (2006). The Drosophila cell corpse engulfment receptor Draper mediates glial clearance of severed axons. *Neuron* **50**, 869-881.
- Marder, E. and Goaillard, J. M. (2006). Variability, compensation and homeostasis in neuron and network function. *Nat. Rev. Neurosci.* **7**, 563-574.
- McGuire, S. E., Le, P. T., Osborn, A. J., Matsumoto, K. and Davis, R. L. (2003). Spatiotemporal rescue of memory dysfunction in Drosophila. *Science* **302**, 1765-1768.
- Miech, C., Pauer, H. U., He, X. and Schwarz, T. L. (2008). Presynaptic local signaling by a canonical wingless pathway regulates development of the Drosophila neuromuscular junction. *J. Neurosci.* **28**, 10875-10884.
- Moline, M. M., Southern, C. and Bejsovec, A. (1999). Directionality of wingless protein transport influences epidermal patterning in the Drosophila embryo. *Development* **126**, 4375-4384.
- Mosca, T. J., Carrillo, R. A., White, B. H. and Keshishian, H. (2005). Dissection of synaptic excitability phenotypes by using a dominant-negative Shaker K+ channel subunit. *Proc. Natl. Acad. Sci. USA* **102**, 3477-3482.
- Neuhaus, E. M., Gisselmann, G., Zhang, W., Dooley, R., Stortkuhl, K. and Hatt, H. (2005). Odorant receptor heterodimerization in the olfactory system of Drosophila melanogaster. *Nat. Neurosci.* **8**, 15-17.
- Packard, M., Koo, E. S., Gorczyca, M., Sharpe, J., Cumberledge, S. and Budnik, V. (2002). The Drosophila Wnt, wingless, provides an essential signal for pre- and postsynaptic differentiation. *Cell* **111**, 319-330.
- Pai, L. M., Orsulic, S., Bejsovec, A. and Peifer, M. (1997). Negative regulation of Armadillo, a Wingless effector in Drosophila. *Development* **124**, 2255-2266.
- Peineau, S., Taghibiglou, C., Bradley, C., Wong, T. P., Liu, L., Lu, J., Lo, E., Wu, D., Saule, E., Bouschet, T. et al. (2007). LTP inhibits LTD in the hippocampus via regulation of GSK3beta. *Neuron* **53**, 703-717.
- Penton, A., Wodarz, A. and Nusse, R. (2002). A mutational analysis of dishevelled in Drosophila defines novel domains in the dishevelled protein as well as novel suppressing alleles of axin. *Genetics* **161**, 747-762.
- Piddini, E., Marshall, F., Dubois, L., Hirst, E. and Vincent, J. P. (2005). Arrow (LRP6) and Frizzled2 cooperate to degrade Wingless in Drosophila imaginal discs. *Development* **132**, 5479-5489.
- Rulifson, E. J., Wu, C. H. and Nusse, R. (2000). Pathway specificity by the bifunctional receptor frizzled is determined by affinity for wingless. *Mol. Cell* **6**, 117-126.
- Salinas, P. C. (2007). Modulation of the microtubule cytoskeleton: a role for a divergent canonical Wnt pathway. *Trends Cell Biol.* **17**, 333-342.
- Sato, K., Pellegrino, M., Nakagawa, T., Nakagawa, T., Vosshall, L. B. and Touhara, K. (2008). Insect olfactory receptors are heteromeric ligand-gated ion channels. *Nature* **452**, 1002-1006.
- Saxena, S. and Caroni, P. (2007). Mechanisms of axon degeneration: from development to disease. *Prog. Neurobiol.* **83**, 174-191.
- Speese, S. D. and Budnik, V. (2007). Wnts: up-and-coming at the synapse. *Trends Neurosci.* **30**, 268-275.
- Spitzer, N. C. (2006). Electrical activity in early neuronal development. *Nature* **444**, 707-712.
- Stewart, B. A., Atwood, H. L., Renger, J. J., Wang, J. and Wu, C. F. (1994). Improved stability of Drosophila larval neuromuscular preparations in haemolymph-like physiological solutions. *J. Comp. Physiol. A* **175**, 179-191.
- Sweeney, S. T., Broadie, K., Keane, J., Niemann, H. and O'Kane, C. J. (1995). Targeted expression of tetanus toxin light chain in Drosophila specifically eliminates synaptic transmission and causes behavioral defects. *Neuron* **14**, 341-351.
- Tessier, C. R. and Broadie, K. (2008). Drosophila fragile X mental retardation protein developmentally regulates activity-dependent axon pruning. *Development* **135**, 1547-1557.
- Toledo, E. M., Colombres, M. and Inestrosa, N. C. (2008). Wnt signaling in neuroprotection and stem cell differentiation. *Prog. Neurobiol.* **86**, 281-296.
- Truman, J. W. and Riddiford, L. M. (2002). Insect developmental hormones and their mechanism of action. In *Hormones, Brain and Behavior* (ed. D. W. Pfaff, A. P. Arnold, S. E. Fahrbach, A. M. Etgen and R. T. Rubin). San Diego, CA: Academic Press.
- van de Wetering, M., Cavallo, R., Dooijes, D., van Beest, M., van Es, J., Loureiro, J., Ypma, A., Hursh, D., Jones, T., Bejsovec, A. et al. (1997). Armadillo coactivates transcription driven by the product of the Drosophila segment polarity gene dTCF. *Cell* **88**, 789-799.
- Wagh, D. A., Rasse, T. M., Asan, E., Hofbauer, A., Schwenkert, I., Durrbeck, H., Buchner, S., Dabauvalle, M. C., Schmidt, M., Qin, G. et al. (2006). Bruchpilot, a protein with homology to ELKS/CAST, is required for structural integrity and function of synaptic active zones in Drosophila. *Neuron* **49**, 833-844.
- Watts, R. J., Hoopfer, E. D. and Luo, L. (2003). Axon pruning during Drosophila metamorphosis: evidence for local degeneration and requirement of the ubiquitin-proteasome system. *Neuron* **38**, 871-885.
- Wayman, G. A., Impey, S., Marks, D., Saneyoshi, T., Grant, W. F., Derkach, V. and Soderling, T. R. (2006). Activity-dependent dendritic arborization mediated by CaM-Kinase I activation and enhanced CREB-dependent transcription of Wnt-2. *Neuron* **50**, 897-909.
- Wicher, D., Schafer, R., Bauernfeind, R., Stensmyr, M. C., Heller, R., Heinemann, S. H. and Hansson, B. S. (2008). Drosophila odorant receptors are both ligand-gated and cyclic-nucleotide-activated cation channels. *Nature* **452**, 1007-1011.
- Yu, C. R., Power, J., Barnea, G., O'Donnell, S., Brown, H. E., Osborne, J., Axel, R. and Gogos, J. A. (2004). Spontaneous neural activity is required for the establishment and maintenance of the olfactory sensory map. *Neuron* **42**, 553-566.
- Yu, X. and Malenka, R. C. (2003). Beta-catenin is critical for dendritic morphogenesis. *Nat. Neurosci.* **6**, 1169-1177.
- Zhao, H. and Reed, R. R. (2001). X inactivation of the OCN1 channel gene reveals a role for activity-dependent competition in the olfactory system. *Cell* **104**, 651-660.
- Zhu, L. Q., Wang, S. H., Liu, D., Yin, Y. Y., Tian, Q., Wang, X. C., Wang, Q., Chen, J. G. and Wang, J. Z. (2007). Activation of glycogen synthase kinase-3 inhibits long-term potentiation with synapse-associated impairments. *J. Neurosci.* **27**, 12211-12220.

**Table S1. Quantitation values for pixel counts of Or22a>GFP terminals in normal and mutant genotypes as plotted in Fig. 2G**

	Or22a>GFP; Or22a>GFP; 8 days PE	Or22a>GFP; Or83b <sup>-</sup> /Or83b <sup>-</sup> ; 8 days PE	Or22a>GFP; Or83b <sup>-</sup> /Or83b <sup>-</sup> UAS Or83b ON at 2 days PE tested at 8 days PE	Or22a>GFP; Or83b <sup>-</sup> /Or83b <sup>-</sup> UAS Or83b ON at 4 days PE tested at 8 days PE	Or22a>GFP; Or83b <sup>-</sup> /Or83b <sup>-</sup> UAS Or83b ON at 6 days PE tested at 8 days PE
Pixel count	40231.3±2890.3	17891.2±3031.2	35682.2±2312.1	31570.9±2787.9	15906.9±2901.2

Pixel count values represent the mean±s.e.m., n=5 for each case.

**Table S2. Quantitation values for pixel counts on Or22a>GFP neurons in normal and mutant genotypes plotted in Fig. 2G**

	Or22a>GFP; 6 days PE	Or22a>GFP; Or83b <sup>-</sup> /Or83b <sup>-</sup> ; 6 days PE	Or22a>GFP/UAS Eag DN, UAS Sh DN; Or83b <sup>-</sup> /Or83b <sup>-</sup> ; 6 days PE	Or22a>GFP/UAS Eag DN, UAS Sh; 6 days PE
Pixel count	45114.2±2200.5	22422.8±2111.2	42679.8±2536.5	44789.12±3010.9

Pixel count values represent the mean±s.e.m., n=5 for each case.

**Table S3. Quantitation values for pixel counts of Or22a>GFP neurons in normal and mutant genotypes as plotted in Fig. 5D**

	Or22a>GFP; 6 days PE	Or22a>GFP; Or83b <sup>-</sup> /Or83b <sup>-</sup> ; 6 days PE	Or22a>GFP/UAS Sgg DN.A81T; Or83b <sup>-</sup> /Or83b <sup>-</sup> ; 6 days PE	Or22a>GFP; Or83b <sup>-</sup> /Or83b <sup>-</sup> fed 10 mM LiCl 6 days PE
Pixel count	45114.2±2200.5	22422.8±2111.2	40281.2±2921.6	37819.1±3100.9

Pixel count values represent the mean±s.e.m., n≥5 for each case.

**Table S4. Quantitation values for pixel counts of Or22a>GFP neurons in mutant and rescue genotypes**

	Mean±s.e.m.	Bar chart plotted in figure
Or22a>GFP; Or83b <sup>-</sup> /Or83b <sup>-</sup> at 6 days PE	25892.09±2908.6	–
Or22a>GFP/UAS Dsh; Or83b <sup>-</sup> /Or83b <sup>-</sup> 6 days PE	35421.2±2309.2	5D
Or22a>GFP/UAS Wg; Or83b <sup>-</sup> /Or83b <sup>-</sup> 6 days PE	34021.2±2908.8	7F
Or22a>GFP/UAS UBP2; Or83b <sup>-</sup> /Or83b <sup>-</sup> 6 days PE	37890.9±2907.2	S6I

n≥5 for each case.

**Table S5. Quantitation values for Wingless levels within the DM2 glomerulus as plotted in Fig. 7C**

	Control (n=5)	5× high K <sup>+</sup> (n=6)
Wg	1869.07±62.9	2277.8±72.2

Values represent the mean±s.e.m.

**Table S6. Quantitation values for pixel counts of Or22a axons within the selected ROI in Fig. S2 as plotted in Fig. S2F**

(A) Or22a>GFP; Or83b <sup>+</sup> /Or83b <sup>+</sup> at 6 days PE (n=5)	24034.3±2345.7
(B) Or22a>GFP; Or83b <sup>-</sup> /Or83b <sup>-</sup> at 2 days PE (n=6)	22409.2±3098.2
(C) Or22a>GFP; Or83b <sup>-</sup> /Or83b <sup>-</sup> at 4 days PE (n=5)	21098.2±2345.4
(D) Or22a>GFP; Or83b <sup>-</sup> /Or83b <sup>-</sup> at 6 days PE (n=6)	11209.8±2909.8
(E) Or22a>GFP; Or83b <sup>-</sup> /Or83b <sup>-</sup> at 8 days PE (n=6)	10109.2±2908.9

Values represent the mean±s.e.m.

**Table S7. Quantitation values for pixel counts of Or22a>GFP axons for mutant and rescue genotypes as plotted in Fig. S3C**

(A) Or22a>GFP>Or83b; Or83b <sup>-</sup> /Or83b <sup>-</sup> at 4 days PE	44509.2±3409.2
(B) Or22a>GFP; Or83b <sup>-</sup> /Or83b <sup>-</sup> at 4 days PE	33670.9±2809.8
(A') Or22a>GFP>Or83b; Or83b <sup>-</sup> /Or83b <sup>-</sup> at 6 days PE	43409.2±3109.8
(B') Or22a>GFP; Or83b <sup>-</sup> /Or83b <sup>-</sup> at 6 days PE	25621.3±3200.09

Values represent the mean±s.e.m., n≥5 for each case.

**Table S8. Quantitation values for Or47b>TNT, with Or47b>IMPTNT-V (control) and Or47b>TNT-G (experimental) for glomerular volume, GFP (as plotted in Fig. S4) and Draper levels (as plotted in Fig. S6)**

	VA6 IMPTNT-V	VA6 TNT-G	VA1v IMPTNT-V	VA1v TNT-G	VA1v IMPTNT-V VA6 IMPTNT-V*	VA1v TNT-G VA1v TNT-G*
Glomerular volume (μm <sup>3</sup> )	4019±45	4137±49	10978±149	8142±181	2.73±0.06	1.97±0.06
GFP		VA1v IMPTNT-V <sup>†</sup> 2747±17			VA1v TNT-G <sup>†</sup> 2784±15	
Draper		VA1v IMPTNT-V <sup>†</sup> 407.4±31			VA1v TNT-G <sup>†</sup> 788.1±31	

n=5 for C and E, except for Draper where n=7 for C and E.

Values represent the mean±s.e.m. C refers to number of control animals and E refers to number of experimental animals.

\*Glomerular volume of VA1v glomerulus normalized to volume of unaffected VA6 glomerulus of the same antennal lobe.

<sup>†</sup>Average intensity per pixel of remaining OSN terminals (judged by GFP staining) in VA1v glomerulus, compared in equivalent ROIs between experimental and control animals.

<sup>‡</sup>Average intensity per pixel of ROI, within VA1v glomerulus (white rectangle in Fig. S6K,M), compared between experimental and control antennal lobes.